IRRADIATION DAMAGE IN GRAPHITE
(The works of Professor B.T.Kelly)

B.J. MARSDEN
Graphite Section, AEA Technology,
Risley, Warrington, Cheshire,
United Kingdom

Abstract

The irradiation damage produced in graphite by energetic neutrons (> 100eV) has been extensively studied because of the use of graphite as a moderator in thermal nuclear reactors. In recent times, graphite has been adopted as the protective tiling of the inner wall of experimental fusion systems and property changes due to fusion neutrons have become important.

The late Professor B.T.Kelly reviewed the work carried out on the irradiation behaviour of graphite since the 1940s. This work is particularly timely as the scale of research into the effects of fission neutrons has been greatly reduced and many of the active researchers have retired.

In recent years, new programmes of work are being formulated for the use of graphite in both the field of high temperature reactor systems and fusion systems. It is therefore important that the knowledge gained by Professor Kelly and other workers is not lost but passed on to future generations of nuclear scientists and engineers.

This paper reviews Professor Kelly's last work, it also draws on the experience gained during many long discussions with Brian during the years he worked closely with the present graphite team at AEA Technology. It is hoped to publish his work in full in the near future.

1. FUNDAMENTALS OF IRRADIATION DAMAGE IN GRAPHITE DUE TO ENERGETIC NEUTRONS

To understand the behaviour of components in fission and fusion systems it is necessary to understand the changes in dimensions and material properties due to displacement of atoms and transmutation products.

In fission systems energies due to source neutrons span over a wide range of energies from less than 1 eV to ~10MeV with a mean energy of ~2MeV. The proposed tritium and deuterium fusion systems produce energies of 14.1MeV.

Transmutation does not play any significant role in property and dimensional changes in fission neutron systems, but this is not certain for higher energy fusion systems.

The process of the creation of crystal lattice defects which produce changes in dimensions is due to elastic and inelastic scattering of carbon atoms. The binding energy of carbon is ~7eV. If the collision is considered to be purely elastic then the maximum energy transferred is $0.284E_n$, where E_n is the initial neutron energy. Neutron nucleus collisions can be considered elastic up to 5.5 MeV and the (n,α) reaction only becomes appreciable for energies above ~9MeV. At these high energies it may also be necessary to account for anisotropic scattering.

Investigation of the energy E_d to produce displaced atoms and the consequent vacant sites has been studied by several authors. The value currently used in the United Kingdom is 40eV. However several authors have proposed values less than 40 eV. Fortunately atomic displacement rates are independent of E_d which is the situation of practical interest.

Simmons[1] proposed a theoretical model for the atomic displacements as:

$$\frac{dN}{dt} = \int \phi(E_n)\sigma(E_n)\bar{\nu}(E_n)dE_n \qquad 1$$

where $\phi(E_n)$ is the neutron flux spectrum, $\sigma(E_n)$ is the elastic scattering cross-section of the carbon nucleus and $\bar{\nu}(E_n)$ is the average number of displacements produced by a collision with a neutron of energy E_n.

This assumption is satisfactory for fission neutrons where the mean energy of the source neutrons is ~2 MeV and only a very small proportion have energies greater than 10 MeV. The source neutrons in Deuterium-Tritium systems have an energy of 14.1 MeV and thus it is necessary to account for anisotropic and inelastic scattering.

Kinchin and Pease[2] were the first to develop a model to estimate the atomic displacement rate in fission systems. The model assumed that the primary neutron-carbon collisions are isotropic with each collision transferring the average energy transfer. The primary knock-on-energy atom loses energy through two mechanisms, the first in collisions with other carbon atoms the second to the electrons. They assumed that all of the energy loss for moving atoms with energies greater than a value designated L_c was electronic in nature and at the lower energies the loss was due to atom-atom collisions. The resulting function $\bar{\nu}(E_n)$ is plotted in Fig. 1.

A complete theory of radiation damage in graphite requires a knowledge of the spatial distribution of displaced atoms as well as their numbers. Simmons dealt with the collision between a moving carbon atom and a lattice atom performing thermal vibrations taking into account the interaction between the electrons and nuclei of the moving and lattice atoms. He used an approximation based on collisions between free atoms with a potential similar to the model due to Bohr.

Simmons showed that at high energies the probability is greater that the energy transferred is a small fraction of the initial energy of the moving atom, while at lower energies the tendency is towards an equal distribution space. The model also showed that the energy of a moving atom at which the rate of energy loss due to collisions is equal to that of the electronic system was 12 eV, which is an estimate for L_c in the Kinchin-Pease model.

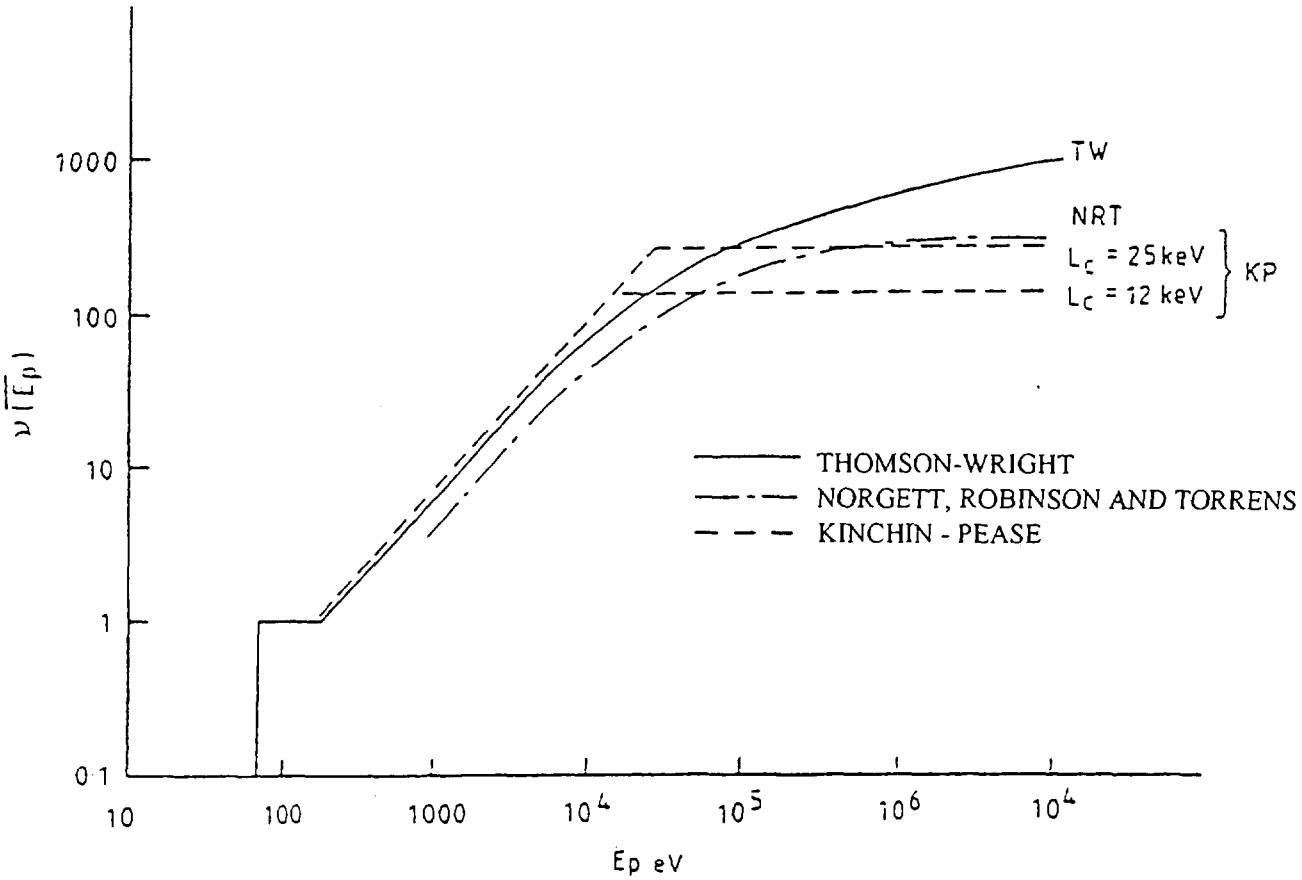

FIGURE 1: COMPARISON OF PRIMARY DISPLACEMENT FUNCTIONS AS CALCULATED BY KINCHIN AND PEASE, THOMSON AND WRIGHT, AND NORGETT, ROBINSON AND TORRENS

For the available data on moving atoms of various energy ranges Simmons was able to show that the average energy of the primary knock on over the range 10^3 to 10^6 eV was 500 eV and that the mean distance between displacement collisions was large compared to the inter-atomic displacements. As a consequence the damage produced by primary knock-on consists of separate groups of displaced atoms, (see Fig. 2). Each group contains less than 10 atoms and the collisions with the displacement groups can be regarded as separate events until the energy falls to less than 100 eV at which the collision becomes comparable with the inter-atomic displacements.

This approach by Simmons provides a method of calculating the number of atomic displacements in carbon and their spatial distribution for fission systems. Calculations of atomic displacement in fusion reactor spectra are more difficult because of the high energy sources.

Prior to consideration of improved methods of calculating atomic displacement rates for fission and fusion reactors it is worth comparing the results with experiments to determine how useful they are. The fundamental reason for such calculations is to predict the dimensional and material property changes of graphite in different neutron spectra.

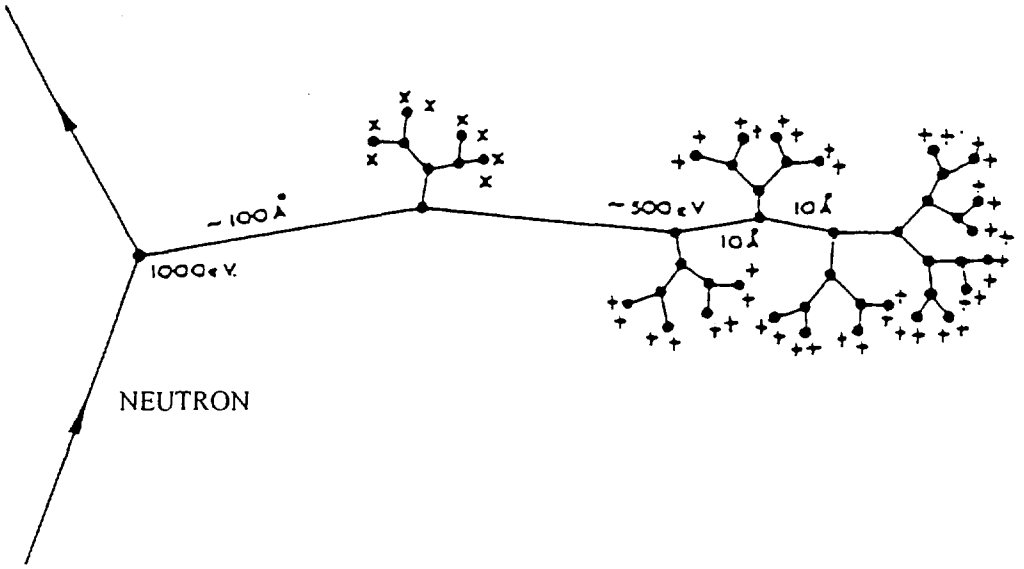

FIGURE 2: DISPLACEMENT CASCADE IN GRAPHITE UNDER NEUTRON IRRADIATION- SCHEMATIC

The changes in a graphite property i may be written:

$$R_i = \frac{1}{P_i}\frac{dP_i}{dt} \propto \int \phi(E_n)\psi_i(E_n)dE_n \qquad 2$$

where $\Psi_i(E_n)$ is a weighting function for the effect of a flux of neutrons $\phi(E_n)$ of energy E_n on the property P_i. In principle Ψ_i may include transmutation as well as classical atomic displacement effects. It can readily be imagined that Ψ_i could depend upon the property considered, obvious possibilities being the number of displaced atoms, the number of displacement groups or perhaps the number of closely spaced groups. Fortunately, in fission neutron systems the number of displaced atoms is an adequate approximation to relate the damaging power of different neutron spectra.

However the distribution of displaced atoms is not truly random. Simmons definition of "damaging power" implies that if identical specimens of graphite are irradiated for the same time at the same temperature in two different neutron spectra, and then show identical property changes, then the damaging power of the two spectra are the same, even if the spectra are different.

It is possible to define a damage flux normalised to some standard such as:

$$\phi_d = \frac{R}{\sigma_d} \qquad 3$$

where σ_d was defined by Simmons[1] with respect to the source neutron flux due to fission e.g.

$$\sigma_d \propto \int_0^\infty \phi(E_n)\sigma(E_n)\bar{\nu}(E_n)dE_n \qquad 4$$

The most generally used normalisation is the neutron spectrum in a Mk III hollow fuel element in the DIDO Materials Test Reactor at the former Atomic Energy Research Establishment, Harwell England. The value of $\bar{\nu}(E_n)$ is due to Thomson and Wright as discussed later.

Calculated damage ratios in different neutron spectra have been compared with experiment by many authors beginning with the work of Bell[3]. It is often assumed that damaging power depends on irradiation dose and temperature. However, it is known that if two identical samples are irradiated to the same dose, but with one sample taking less time than the other, the sample which is irradiated slower will exhibit more damage. This is because the slower irradiation allows more time for thermal processes to occur.

The rate effect can be accounted for using the concept of equivalent temperature as given below:

$$\frac{1}{\theta} - \frac{1}{T_i} = \left(\frac{k}{E}\right) ln\left(\frac{A}{A_s}\right) = \left(\frac{k}{E}\right) ln\left(\frac{\phi_d}{\phi_s}\right) \qquad 5$$

where θ K is the "Equivalent Temperature" which would be required in a flux producing a standard displacement rate A_s sec^{-1} to produce the same observed property changes as a function of damage dose as those observed at a temperature T_i K, displacement rate A sec^{-1}. Boltzmann's constant is denoted by k.

The activation energy E is determined experimentally and various values have been proposed. In the UK 1.2eV is now used for low temperature, low dose effects and 3 eV for high dose effects, however some uncertainty still exists as to the appropriate value.

Simmons[1] compared the experimental and calculated ratio of damage as derived from changes in electrical resistivity to the flux measured by the N_i $^{58}(n,p)$ Co^{58} reaction with a cross-section of 0.107×10^{-24} cm^2 and obtained a series of ratios for various facilities. The calculations were based on the Kinchin-Pease model using a value of L_c of 25 eV.

The first proposal for an improved model was made by Thomson and Wright[4]. The energy E_D out of an initial energy E_p was calculated from:

$$E_D = \int_0^{E_p} \frac{\left(\frac{dE}{dx}\right)_c}{\left\{\left(\frac{dE}{dx}\right)_c + \left(\frac{dE}{dx}\right)_e\right\}} dE \qquad 6$$

where $(dE/dx)_c$ is the rate of energy loss/unit path length due to collisions.

$(dE/dx)_e$ is the rate of energy loss/unit path length due to electronic processes.

This was used to calculate the average number of displacements for a primary knock-on of energy E_p. The function $\bar{\nu}(E_p)$ is shown in Fig. 1.

The new model did not make a significant difference to the calculated ratios of displacement rate to activation normalised to the standard position which was now changed to a spectrum associated with the DIDO hollow fuel element. As a consequence of this work the IAEA[5] in 1972 recommended that graphite damage doses in fission reactors should be calculated using the Thomson and Wright model with the spectrum in the DIDO hollow fuel element as a standard.

The damage doses are generally expressed in these units for experiments carried out in UK, Japan and Germany, but in the USA and Russia it was noted that relative damage rates could be accurately estimated by taking the neutron flux with energies above some value E_n. Conversion factors between various dose and flux units are given in Table 1.

Table 1 Conversion of Various Graphite Damage Dose Units to Equivalent DIDO Nickel Dose

Dose or Flux Units and Original Source	Multiply by
Equivalent DIDO Nickel Dose (EDND or DNE) UKAEA	1.0
Equivalent Fission Dose (33) UKAEA	0.547
Calder Equivalent Dose (MWd/Ate) UKAEA	1.0887×10^{17}
[1]BEPO Equivalent Dose UKAEA	0.123 (Morgan gives 0.962±0.01)
Neutron dose $n.cm^{-2}$ ($E > 0.05$ MeV) USA	0.5
Neutron dose $n.cm^{-2}$ ($E > 0.18$ MeV) USA	0.67
Neutron dose $n.cm^{-2}$ ($E > 1.0$ MeV) USA	0.9

Various improvements have been made to the Thomson and Wright model, by various authors[6] taking account of inelastic scattering, anisotropic scattering and electronic energy loss in the secondary and later knock-ons. One of these models, the Norgett/Robinson/Torrens or NRT model is given in Fig. 1.

Strictly speaking this model is unsatisfactory for collisions with neutron energy greater than 11 MeV due to inelastic effects.

Table 2 gives a comparison of displacement cross-section for 14.1 MeV neutrons in graphite.

Three of the results are similar but both Morgan's and Huang and Ghoniem's are significantly higher even when corrected for the difference in E_d and the displacement efficiency. The reasons for these differences are not clear but must lie in the treatment of the cross-sections.

[1] Note BEPO equivalent dose was based on thermal neutron dose which is not really suitable for the purpose.

Table 2

Comparison of the Displacement Cross-section for 14.1 MeV Neutrons in Graphite

Source	Reactions included	dpa/n.cm^{-2} (x 10^{-22})
Robinson (1969)	(n,2n)	2.34
Morgan (1974)	(n,α)	5.18
Gabriel et al (1976)	(n,α)	3.76
Adams (1987)	(n,α),(n,n')	2.71
Huang and Ghoniem (1993)	(n,α),(n,p),(n,λ)	4.9

The relative damage power in high energy systems must eventually be determined experimentally. Work in this area suggests that high energy neutrons produce greater energy than would be expected from displacement models and also the damage differs in quality.

The current situation appears to be that it is possible in fission systems to estimate the relative damage rates in different reactor spectra with some degree of accuracy. However in fusion spectra the situation is more complex - quite large differences exist in displacement cross sections for high energy neutrons estimated by various authors. Thus, estimates in spectra dominated by source neutrons are not likely to be accurate. However the situation is much better in the substantially degraded spectra which are likely to be found in most of the graphite components in a fusion reactor.

High energy neutrons in fusion reactors produce transmutation effects to a much greater degree than in fission systems. In particular the transmutation to helium or other elements may have an important effects on property changes. Various authors have studied the effect of transmutation in graphite, however more study is desirable.
It would be sensible for all future data for high energy systems to be expressed in a displacement scale using an agreed set of input data. (Conditional on transmutation effects being unimportant).

It is highly desirable that a better absolute displacement rate scale should be achieved which requires further studies of the displacement energies, particularly the angular and temperature dependencies. The best representation of the electronic energy loss data and neutron cross-sections requires agreement and proper allowance made for inelastic and anisotropic scattering. Calculations for a particular irradiation should also give best estimates of the transmutation rates, particularly the production of helium.

2. DIMENSIONAL CHANGES IN GRAPHITE AND THE THERMAL EXPANSION COEFFICIENT

Irradiation of graphite with energetic neutrons leads to dimensional changes of considerable magnitude which must be accommodated for in reactor design.

Graphite may be considered to be an aggregate of crystallites of identical properties. The irradiation behaviour of the crystallite is that they grow perpendicular to the basal planes and shrink parallel to the planes.

In free crystals there are two distinct measurements of crystal dimensional change. The mean inter-atomic displacement parallel and perpendicular to the hexagonal axis (macroscopic scale) and the changes to the embedded gauge length in each crystallite (microscopic scale). The second measurement is described here.

Simmons[1] obtained theoretical relationships between the thermal expansion coefficient and the dimensional change rates as follows:

The rate of dimensional change with dose, $dG/d\gamma$, in direction 'x' may be expressed in terms of the crystallite dimension changes perpendicular to the basal plane, direction 'c' and parallel to the basal plane direction 'a', as:

$$\frac{dGx}{d\gamma} = A_x \frac{1}{X_c}\frac{dX_c}{d\lambda} + (1 - A_x)\frac{1}{X_a}\frac{dX_a}{d\lambda} \qquad 7$$

Also the thermal expansion coefficient α in direction 'x' can be expressed in terms of the crystallite thermal expansion coefficients as:

$$\alpha_x = A_x\alpha_c + (1 - A_x)\alpha_a \qquad 8$$

The coefficient A_x is a function of irradiation dose.

For a polycrystalline graphite given the thermal expansion coefficient of the graphite crystal α_c = 26 x 10^{-6} K^{-1}, α_a = -1.1 x 10^{-6} K^{-1} and data for two directions x which give significantly different dimensional changes and expansion coefficients these equations can be solved for the two rates of crystal dimensional change (assuming that α_c and α_a are not changed by irradiation).

Direct measurements of $\Delta X/X_c$ and $\Delta X/X_a$ can be made using pyrolytic graphite or crystal flakes, as given in Fig. 3. The growth perpendicular to the basal plane and shrinkage parallel to the basal plane continues over all measured doses.

The lower temperature data shows large volume changes at low dose where as the higher temperature data shows dimensional changes at constant volume.

It is useful to define a parameter:

$$\delta = \frac{\frac{1}{X_a}\frac{dX_a}{d\gamma}}{\frac{1}{X_c}\frac{dX_c}{d\gamma}} \qquad 9$$

which varies with dose and temperature. A value of δ =-0.5 corresponds to changes at constant volume.

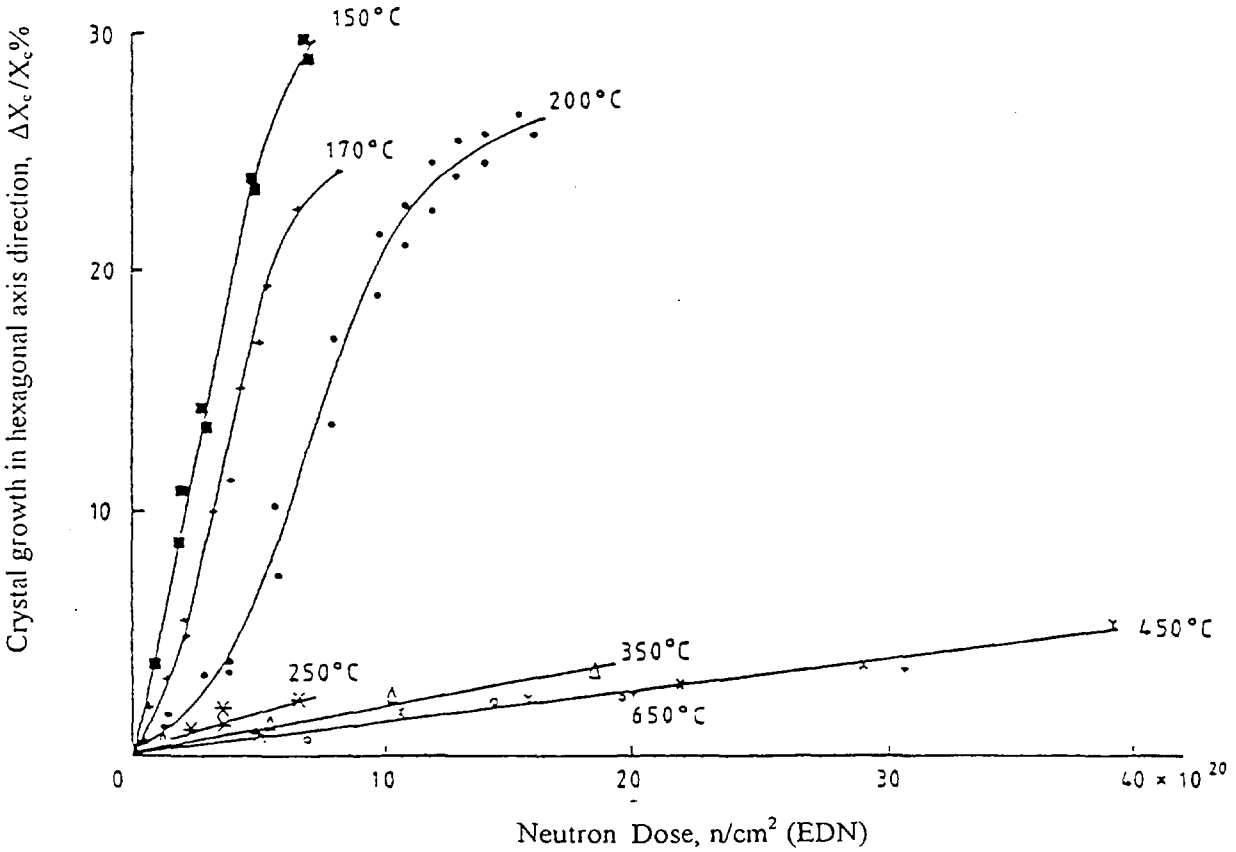

(a) Perpendicular to the Basal Planes

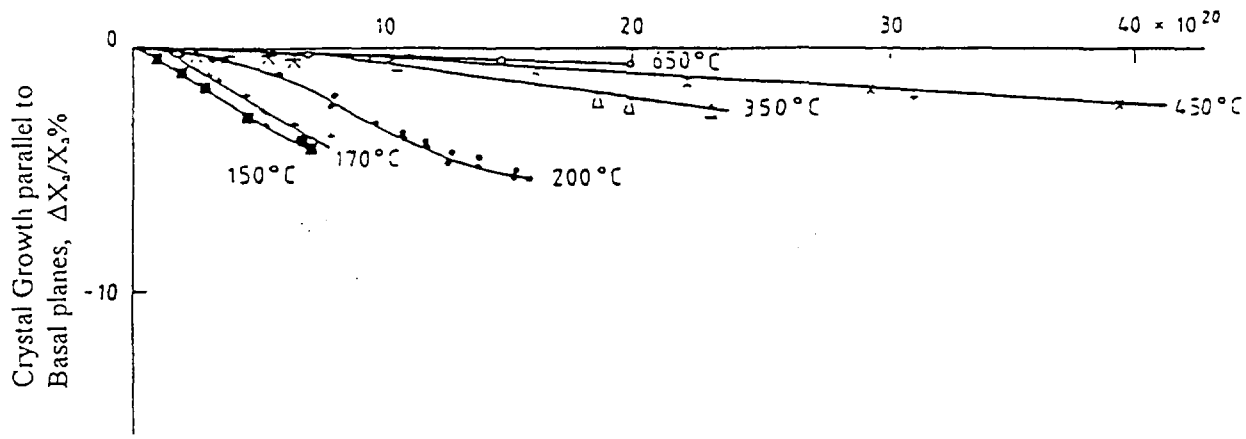

(b) Parallel to the Basal Plane

FIGURE 3: DIMENSIONAL CHANGES OF PYROLYTIC GRAPHITE (LOW TEMPERATURE)

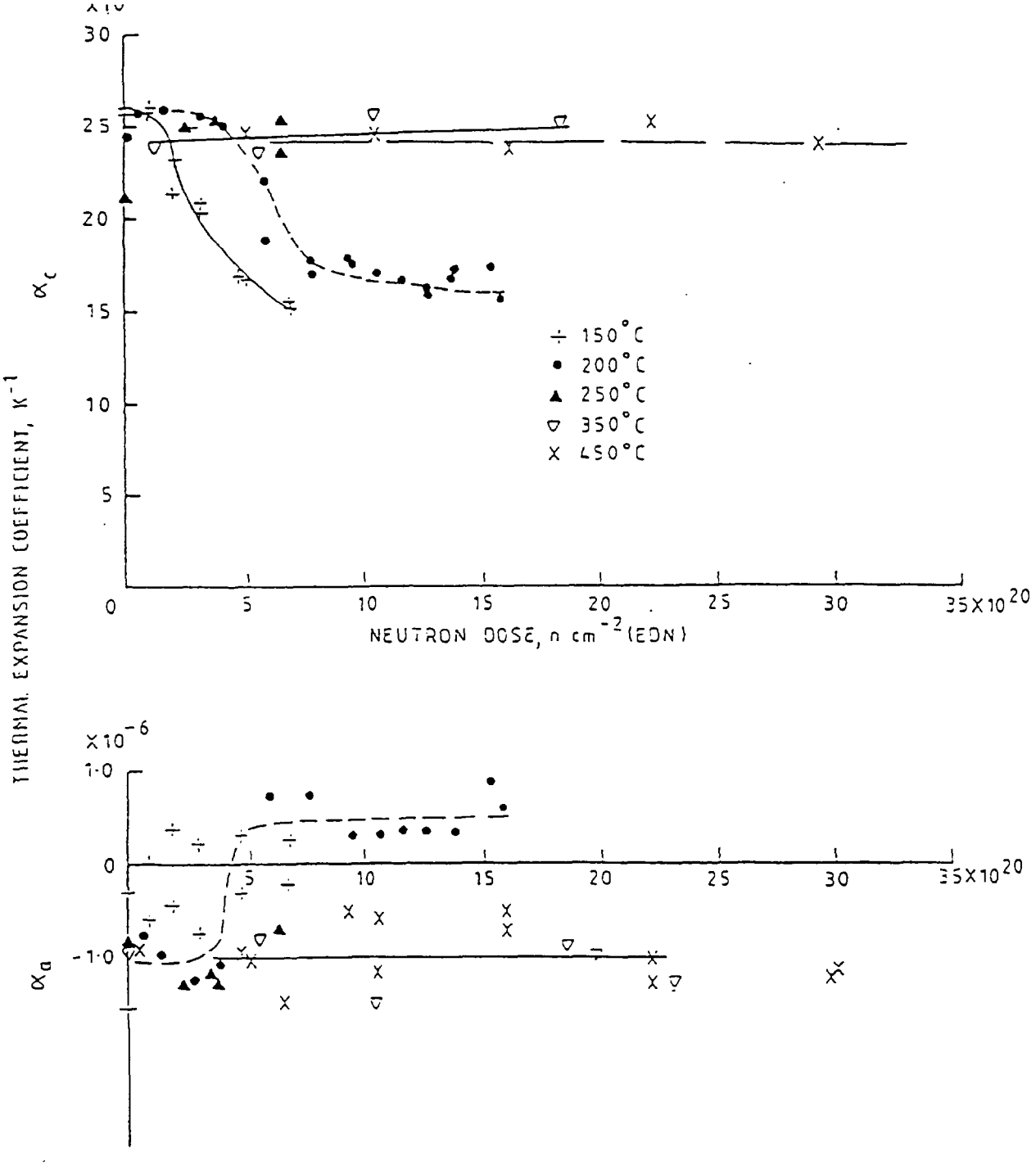

FIGURE 4: PRINCIPAL THERMAL EXPANSION COEFFICIENTS OF HIGHLY ORIENTED PYROLYTIC GRAPHITE AT VARIOUS IRRADIATION TEMPERATURES

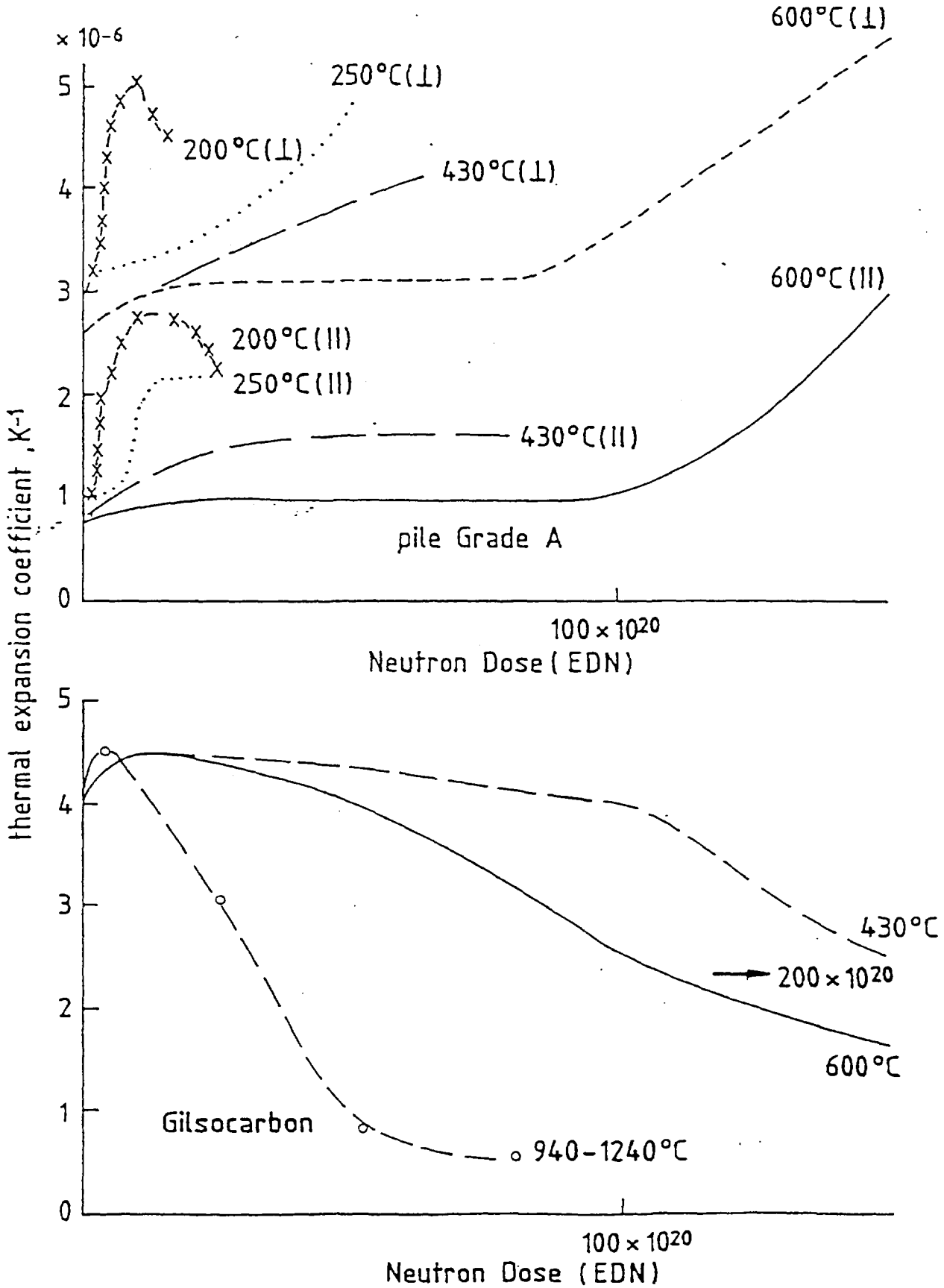

FIGURE 5: THEMAL EXPANSION COEFFICIENT V's DOSE FOR PILE GRADE A AND GILSOCARBON GRAPHITE

For irradiations below 300°C, where δ varies with dose changing from a low value and increasing to constant volume conditions, the crystallite changes in the thermal expansion coefficient α_a and α_c also undergo significant changes, see Fig. 4.

The irradiation changes in the coefficient of thermal expansion in polycrystalline graphite is quite complex and not well understood, particularly at low irradiation temperatures. The data for Pile Grade A graphite is given in Fig. 5.

The dimensional change rate can be related(equation 7,8) to the coefficient of expansion using the relationships due to Simmons as:

$$\frac{dG_x}{d\gamma} = \left[\frac{1}{X_c}\frac{dX_c}{d\gamma} - \frac{1}{X_a}\frac{dX_a}{d\gamma}\right]\frac{\alpha_x}{\alpha_c - \alpha_a} - \left[\frac{1}{X_c}\frac{dX_c}{d\gamma} - \frac{1}{X_a}\frac{dX_a}{d\gamma}\right]\frac{\alpha_a}{\alpha_c - \alpha_a} + \frac{1}{X_a}\frac{dX_a}{d\gamma}$$

or at low irradiation doses, at which the rates can be considered to be constant.

$$\frac{dG_x}{d\gamma} = A_x\alpha_x + B$$

10

There is therefore a value of α_x for which the graphite is dimensionally stable and this observation was used to specify graphites with improved dimensional behaviour for us in the UK Advanced Gas Cooled Reactors.

The definition of δ requires that all the graphite crystallites behave the same way under irradiation. The pyrolytic graphite showed that this is true for irradiations below 600°C but not at higher temperatures where δ changes with irradiation dose.

The relationship between dimensional change and thermal expansion coefficient was studied by Kelly, Martin and Nettley[7]. They showed that the values for A_x were the same for both relationships up to a critical dose γ^* after which the value becomes larger for dimensional change than thermal expansion coefficient. This was attributed to the generation of porosity.

A large volume of data has been accumulated on a few nuclear graphites over a wide range of irradiation temperatures. Data for Pile Grade A and Gilsocarbon graphite is given in Figs. 6 and 7.

2.1. *Theory of dimensional changes in irradiated graphite*

Kelly developed the relationship between dimensional change and CTE to include an additional porosity term f_x, furthermore Kelly et al. proposed that the structural dependent factors A_x and f_x depend on X_T, defined as:

$$X_T = \left(\frac{\Delta X}{X_c} - \frac{\Delta X}{X_a}\right) \qquad 11$$

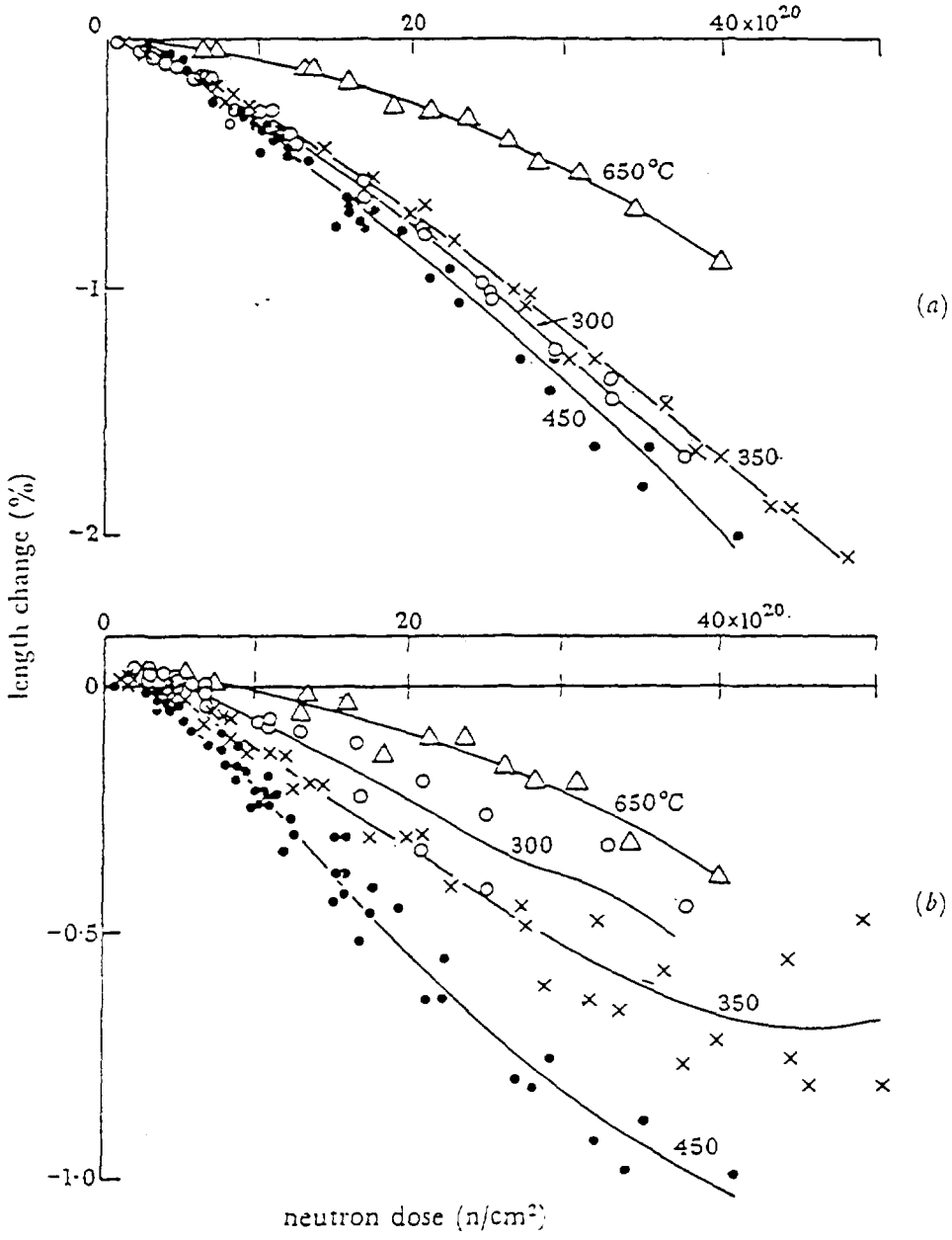

FIGURE 6: DIMENSIONAL CHANGES INDUCED IN 'PGA' GRAPHITE BY NEUTRON IRRADIATION IN THE TEMPERATURE RANGE 300 TO 650°C.
(a) PARALLEL TO EXTRUSION; (b) PERPENDICULAR TO EXTRUSION

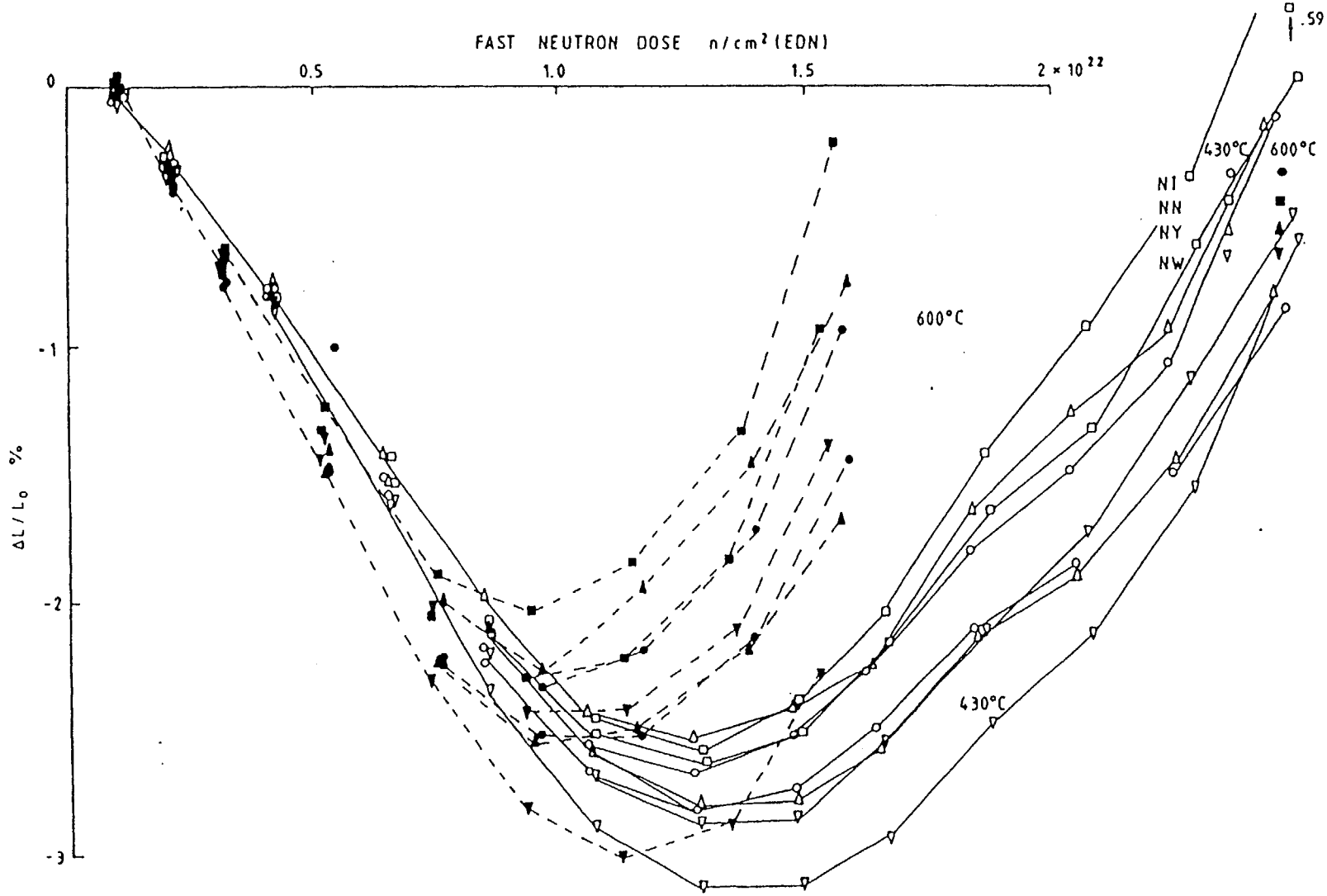

FIGURE 7: DIMENSIONAL CHANGES OF 'CAGR' MODERATOR GRAPHITE IN 'PLUTO' (S2) AT 430 AND 600°C.

Thus including the porosity term and integrating equation 10 we obtain an expression for dimensional change:

$$G_x = \int A_x(X_T)\frac{dX_T}{d\gamma}d\gamma + \frac{\Delta X_a}{X_a} + F(X_T) \qquad 12$$

where

$$F_x = \int f_x d\gamma \qquad 13$$

This relationship can be used to develop a set of simultaneous equations for an anisotropic graphite such as Pile Grade A.

$$\begin{aligned} f_1(X_T) &= (G_\perp - G_{11}) = \int (A_\perp - A_{11})\frac{dX_T}{d\gamma}d\gamma + (F_\perp - F_{11}) \\ f_2(X_T) &= (2G_\perp - G_{11}) - 3\frac{\Delta X_a}{X_a} = \int (2A_\perp - A_{11})\frac{dX_T}{d\gamma} + (2F_\perp - F_{11}) \end{aligned} \qquad 14$$

The symbol '$\perp$'and '$\parallel$' refers to directions perpendicular and parallel to extrusion. Brocklehurst and Kelly used these equations and showed that the form of f_1 and f_2 was essentially the same for irradiations at 200°C and 600°C although the macroscopic dimensional change behaviour is significantly different. These dependencies on X_T extended well into the pore generation regime.

For isotropic graphite $f_1 = 0$ and equation 14, for f_2, may be written as:

$$f_2(X_T) = \frac{\Delta V}{V} - 3\frac{\Delta X_a}{X_a} = 3\int A_x \frac{dX_T}{d\gamma}d\gamma + F_v \qquad 15$$

where $\Delta V/V$ is the bulk volume change of graphite and F_v is the pore volume generation.

This relationship may be simplified to:

$$f_2(X_T) = \frac{\Delta V}{V} - \frac{\Delta V_c}{V_c} + X_T \qquad 16$$

or

$$\frac{\Delta V}{V} = \phi(X_T) + \frac{\Delta V_c}{V_c} \qquad 17$$

thus relating the bulk volume change to the crystal volume change via a function of X_T.

For temperatures in the AGR range 400-450°C $\Delta V_c/V_c$ is approximately zero and $\Delta V/V$ is a unique function of X_T. Therefore $\phi(X_T)$ can be determined from irradiations in this range.

It is therefore possible to analyse data for irradiation temperatures greater than 600°C where the crystallite dimensional changes depend upon the crystal perfection. (This is possible if the crystallites in the material behave the same.)

The crystal volume change, if δ is constant in dose, can be written:

$$\frac{\Delta V_c}{V_c} = \frac{\Delta X_c}{X_c} + 2\frac{\Delta X_a}{X_a} = X_T\left[\frac{1+2\delta}{1-\delta}\right] \qquad 18$$

Equation 18 can be used along with equation 17 to plot $\Delta V/V$ against X_T, using values of $\phi(X_T)$ from irradiations at 450°C, for various values of δ.
These relationships can then be used to obtain:

$$\frac{\Delta V}{V} = 0, \quad X_T$$
$$\frac{1}{V}\frac{dV}{d\gamma} = 0, \quad X_T \qquad 19$$

for different levels of porosity generation.

This type of analysis can be used to predict the behaviour of graphite irradiated at different temperatures from one set of irradiation data carried out at ~450°C. However more work is still required in this area.

3. STORED ENERGY AND THE THERMOPHYSICAL PROPERTIES OF GRAPHITE

3.1. Stored energy

Crystal lattice defects introduced by fast neutron irradiation increase the energy of the graphite crystals. Increasing the temperature above that at which the defects were produced allows the defects to rearrange themselves, the excess energy being produced as heat. This stored energy is often referred to as Wigner energy after the scientist who first proposed its existence.

In graphite irradiated at room temperature, very large levels of stored energy can accumulate, values of up to 2,700 J/g (645 cals/g) have been recorded[1]. If all this energy were released as heat it would lead to temperature rises of in the region of 1500°C. However, in air, before this temperature is reached the graphite would start to thermally oxidise.

The stored energy content of graphite can be measured in a number of ways[1]. The most usual are to measure total stored energy content by combustion of the graphite in a high pressure oxygen in a bomb calorimeter, or to measure the rate of release of stored energy using the linear rise method.

The total stored energy in a sample can be related to the fractional change in thermal conductivity by the empirical equation[3]:

$$S = A\left[\frac{K_o}{K} - 1\right] \quad \text{J/g} \qquad 20$$

The constant A in this equation is dependent on the graphite and the irradiation conditions. For experiments carried out at temperatures above 150°C in various Material Test Reactors (MTRs) a value of 6.25 cal/g (26.2 Joules/g) was obtained. However, this constant may not apply to other graphites, or other reactor conditions.

There is also a relationship between total stored energy and the value of *dS/dT* at 400°C.

$$S = B\left[\frac{dS}{dT}\right]_{400} \quad \text{J/g} \qquad 21$$

The constant B was found to be 1670. However, again this empirical relationship was derived from tests in many MTRs and may not apply to other graphites irradiated in differing conditions.

In safety assessments it is not the total amount of stored energy that is of prime concern but the rate of release of this energy with temperature rise and the temperature at which this release rate becomes significant.

Fig. 8 gives some rate of release measurements for graphite irradiated at low temperature. The specific heat of graphite is also included on this curve. The prominent dS/dT peak around 200°C rises above the specific heat. The significance of this is that whilst the rate of release curve is below the specific heat curve, heat must be applied to raise the temperature of the graphite, but when the curve rises above the specific heat curve the graphite is self heating

However this is not the complete picture, if the linear rise experiment is carried out to very high temperatures another peak is formed at approximately 1500°C, see Fig. 9.

The 200°C peak changes with irradiation dose, at first to a sharp peak reaching about 1.0 cal/g/°C, then falling sharply to an almost flat rate at doses greater than 2.5 x 10^{20} n/cm^2 EDND[8]. However, the plateau in the *dS/dT* curve between the 200°C peak and the 1500°C peak, rises with further irradiation towards the specific heat curve, see Fig. 10. There was a concern that for graphites irradiated to high doses at these low temperatures the intermediate plateau may have risen above the specific heat thus allowing a spontaneous increase in temperature to 1500°C.

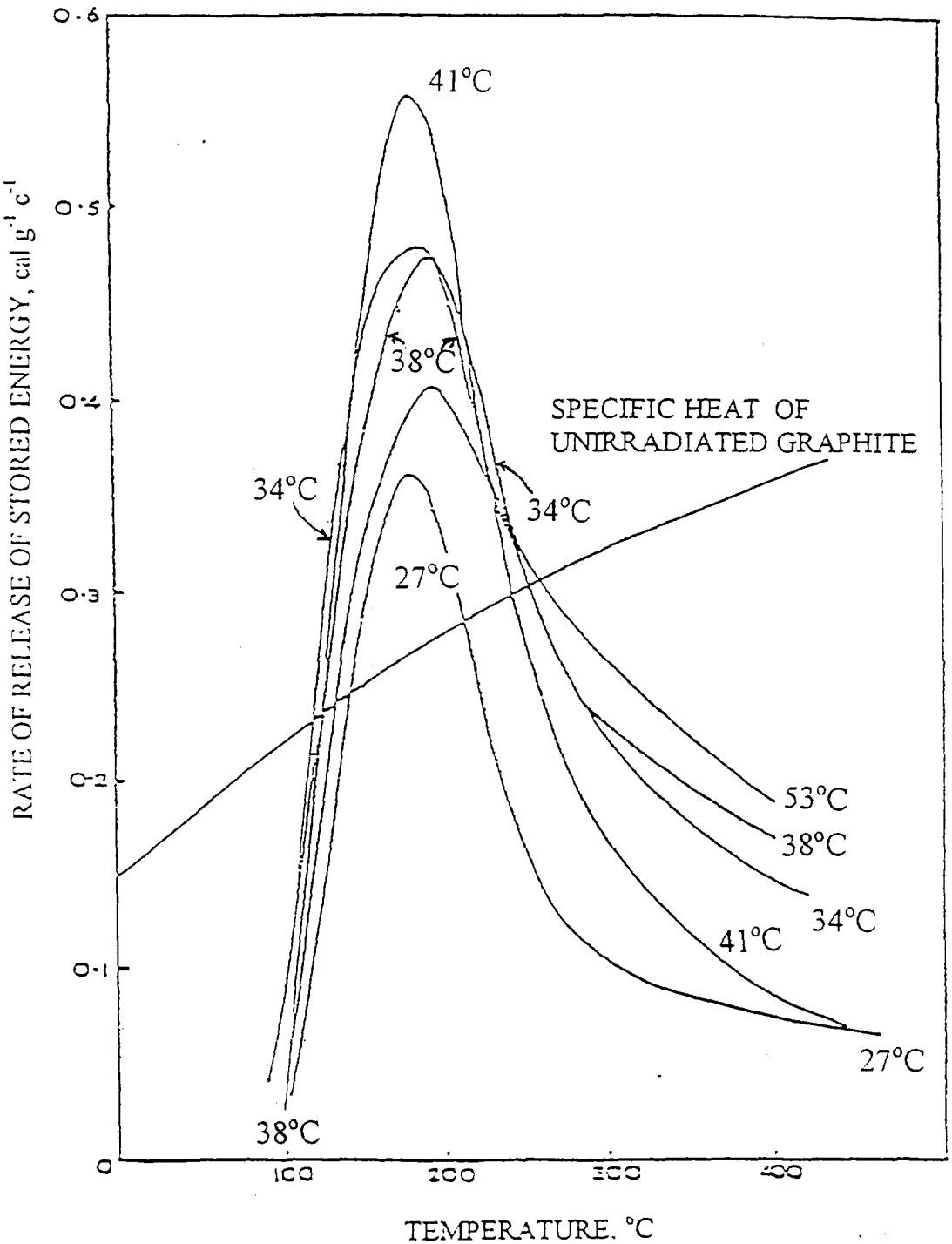

FIGURE 8: LINEAR RISE CURVES FOR GRAPHITE IRRADIATION BELOW 150°C

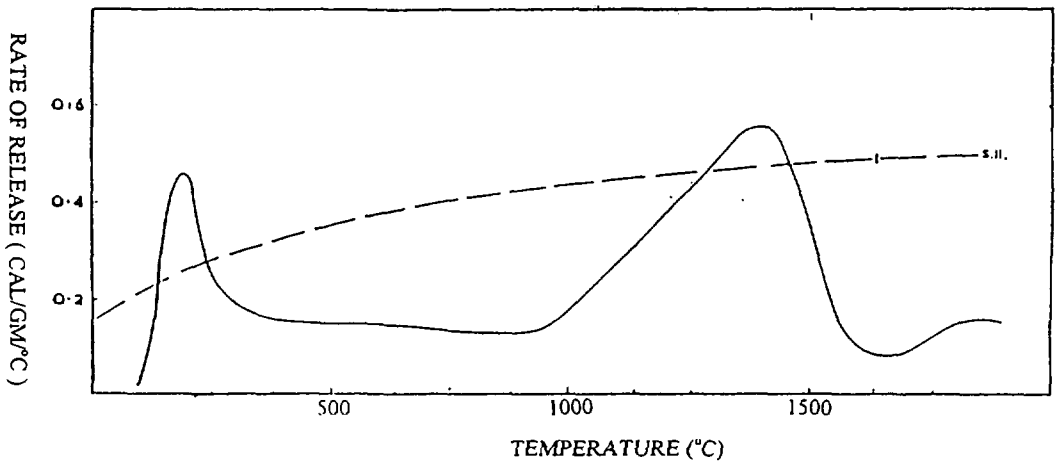

FIGURE 9: RATE OF RELEASE OF STORED ENERGY WITH TEMPERATURE (SCHEMATIC)

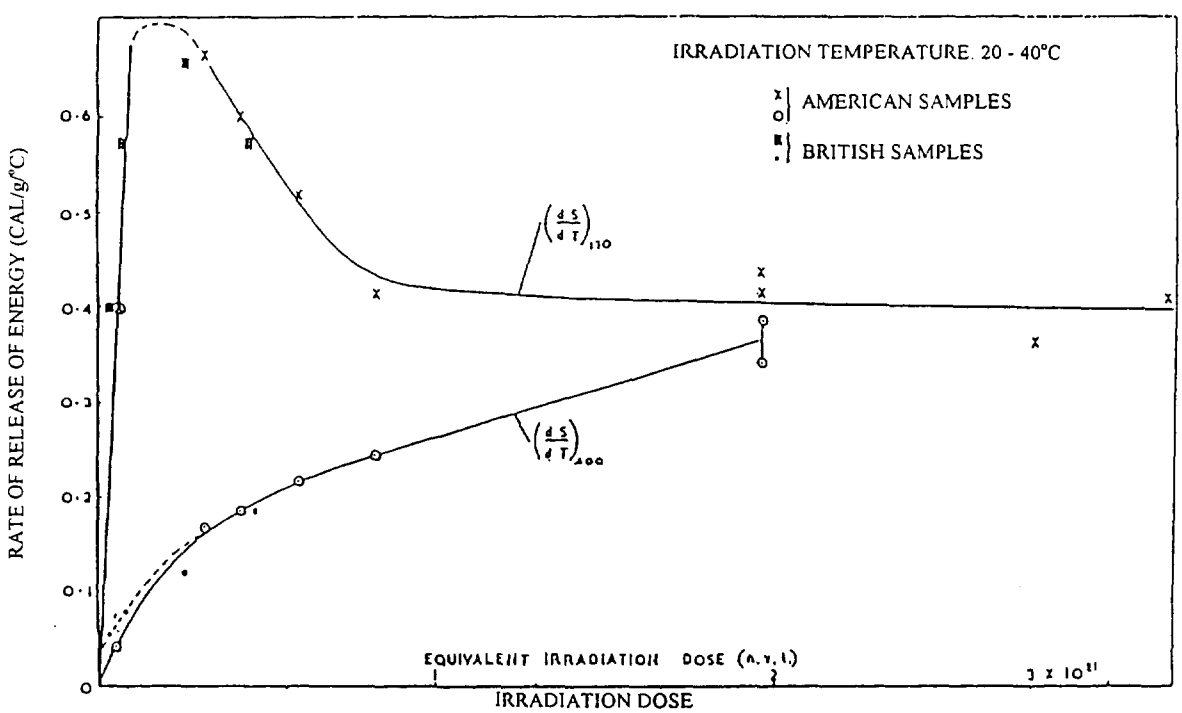

FIGURE 10: BUILD-UP OF ENERGY RELEASE RATE IN HANFORD COOLED TEST HOLE SPECIMENS AND IN WINDSCALE IRRADIATED SPECIMENS.

The rate of release of stored energy from a sample can be described by:

$$\frac{dS}{dt} = f(S)e^{-\frac{E(S)}{kT}} \quad \text{J/g} \qquad 22$$

where $E(S)$ (eV) is the activation energy as a function of stored energy remaining in the sample, T (°K) is the temperature, k is Boltzmann's constant and $f(S)$ is a function which characterises the state of the sample.

Ignoring any exothermic heat generated due to graphite oxidation, the heat produced during the release of stored energy is a balance between the heat generated by the release of the stored energy and the heat lost (or gained) from the environment. This can be expressed by a heat balance equation as:

$$C_P(T)\delta T = -\frac{dS}{dt}\delta t + \frac{dh}{dt}\delta t \quad \text{J/g} \qquad 23$$

where $C_p(T)$ is the specific heat and dh/dt is the rate of heat gained or lost to the environment.

The heat loss to the environment can usually be calculated based on the heat transfer and geometry of the sample or component of interest and is likely to be a function of temperature and time.

The problem is therefore to determine dS/dT. There are various models which deal with the kinetics of the release of stored energy: Two of these models are discussed below.

3.1.1. Variable activation energy model

The functions $f(S)$ and $E(S)$ can be derived from linear rise experiments using assumptions about activation energy as a function of temperature and linear rise rate.

It is important to account for the increase in thermal conductivity as the annealing proceeds as can be seen from equation 20.

It is possible to obtain $f(S)$ and $E(S)$ from a pair of linear rise experiments taken at different rates, for example 2.5 °C/min and 25 °C/min. From these experiments rate of release curves can be derived:

$$\left(\frac{dS}{dt}\right)_1 = f(S)e^{-\frac{E(S)}{kT_1}}$$
$$\left(\frac{dS}{dt}\right)_2 = f(S)e^{-\frac{E(S)}{kT_2}} \qquad 24$$

These equations can then be combined to give:

$$\frac{E(S)}{k}\left(\frac{1}{T_1}-\frac{1}{T_2}\right)=ln\left(\frac{dS}{dt_1}\right)-ln\left(\frac{dS}{dt_2}\right) \qquad 25$$

Thus $E(S)$ may be obtained and then $f(S)$ calculated. However, it is not necessary to calculate $f(S)$ as the rate of release in the component can be given as:

$$\frac{dS}{dt}=\left(\frac{dS}{dt}\right)_1 e^{-\frac{E(S)}{k}\left(\frac{1}{T}-\frac{1}{T_1}\right)} \quad J/g/^\circ C \qquad 26$$

3.1.2. Constant activation model

Unfortunately, rate of release measurements taken at different rates are not always readily available. A pessimistic approximation can be made by assuming a constant activation energy. In most of the early work[9] a value of 1.7 eV was widely used. However, recent unpublished work by Simmons suggests a constant value of 1.2 eV may be more appropriate. Thus, the rate of release equation becomes:

$$\frac{dS}{dt}=f(S)e^{-\frac{E}{kT}} \quad J/g/^\circ C \qquad 27$$

3.1.3. Constant frequency factor model

This model was proposed by Vand[10] and developed later by Primak[11]. In its simplest form it assumes that the energy release process for each group of defects obeys first order kinetics. Thus for a group with activation energy E at constant temperature T:

$$\frac{dS(E,t)}{dt}=-\upsilon S(E,t)e^{-\frac{E}{kT}} \qquad 28$$

where υ is a constant (or variable) frequency factor which is in practice altered to suit the experimental data.

3.2. Thermal Conductivity

The thermal conductivity of a graphite crystal has two principal tensors, measured perpendicular and parallel to the basal plane. In the range of interest the conductivities are both dominated by lattice vibrations (phonons). The conductivity is much higher parallel to the basal plane than perpendicular to the plane and in

polycrystalline graphite the basal conductivity dominates. It is therefore possible to define the thermal conductivity K in some arbitrary direction x as:

$$K_x = \frac{K_a}{\beta_x} \qquad 29$$

where β_x is a constant and K_a is the basal conductivity. The thermal resistance in the basal plane can be regarded as the sum of the thermal resistance due to three effects, scattering at the crystal boundary, $1/K_B$, phonon scattering, $1/K_u$ and due to lattice defects, $1/K_D$.

$$\frac{1}{K_a} = \frac{1}{K_B} + \frac{1}{K_U} + \frac{1}{K_D} \qquad 30$$

The effect of irradiation is to increase the latter effect.

The temperature dependence on the thermal resistivity of unirradiated graphite is to reduce the resistivity, however this temperature dependence is modified by irradiation. It has been shown that this modification in temperature dependence can be normalised to unity at 300K for irradiations below 450°C.

For irradiations below 450°C the thermal conductivity $K(\gamma,T_m)$, at some temperature T_m, is usually expressed as:

$$K_x(\gamma,T_m) = K(0,T_m)\left[1 + f\delta(T_m)\left\{\frac{K_x(0,T_m)}{K_x(0,300)}\right\}\right] \qquad 31$$

where f is the fractional change in thermal resistivity due to irradiation, $\delta(T_m)$ is the irradiation induced change in the temperature dependence of thermal resistivity and $K_x(0,T_m)/K_x(300,T_m)$ is the normalised unirradiated temperature dependence of thermal conductivity.

Fractional changes in thermal conductivity for Pile Grade A are given in Fig. 11. In the UK these changes are assumed to be the same perpendicular and parallel to the direction of extrusion.

4. MECHANICAL PROPERTIES AND IRRADIATION CREEP OF GRAPHITE

Unirradiated graphites are near brittle materials with a low elastic modulus ~10GPa. The stress-strain curves are highly non-linear and exhibit a high degree of hysteresis. Strain to failure is a magnitude higher in compression than in tension.

Extruded or moulded polycrystalline graphite possess an axis of symmetry parallel to the extrusion or pressing direction. The same symmetry applies to highly

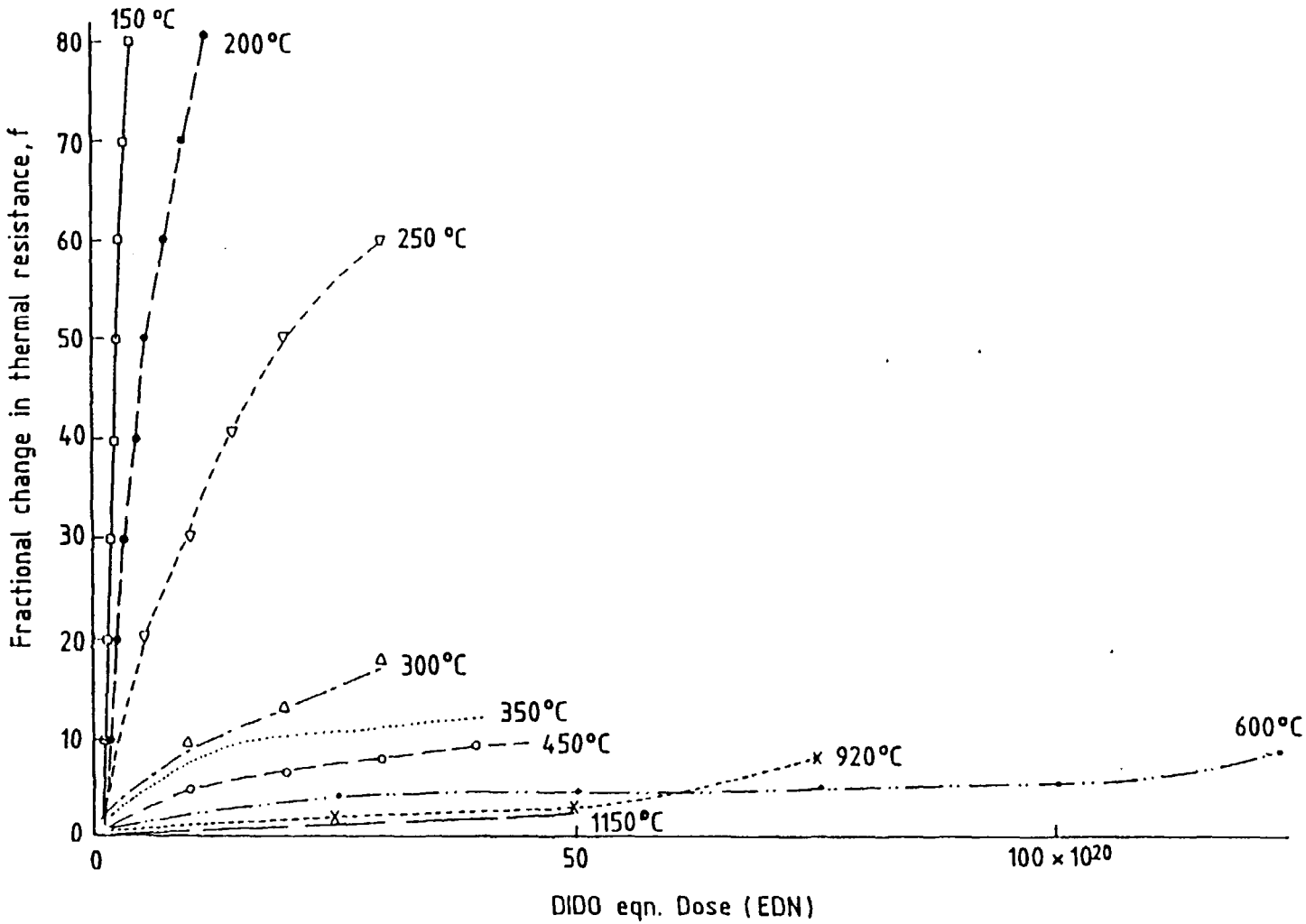

FIGURE 11: FRACTIONAL CHANGES IN THERMAL RESISTANCE OF PILE GRADE 'A' GRAPHITE

orientated pyrolytic graphite. In both these cases five elastic components of moduli are required to describe the elastic behaviour of the material.

In terms of compliance this gives:

$$\begin{aligned} e_{xx} &= S_{11}T_{xx} + S_{12}T_{yy} + S_{13}T_{zz} \\ e_{yy} &= S_{12}T_{xx} + S_{11}T_{yy} + S_{13}T_{zz} \\ e_{zz} &= S_{13}T_{xx} + S_{13}T_{yy} + S_{33}T_{zz} \\ e_{zx} &= S_{44}T_{zx} \\ e_{zy} &= S_{44}T_{zy} \\ e_{xy} &= 2(S_{11} - S_{12})T_{xy} \end{aligned} \qquad \ldots\ldots\ 32$$

In the case of isotropic graphites such as Gilsocarbon only three terms are required. The elastic compliance for a perfect crystal are given in Table 3 along with the elastic compliance for Pile Grade A and Gilsocarbon.

Table 3 Elastic compliances and constants for a perfect graphite Crystal

Elastic Compliance	Pile Grade A (Anisotropic) $m^2/N \times 10^{-13}$	Gilsocarbon (Isotropic) $\times 10^{-13}\ m^2/N$	Perfect crystal $\times 10^{-12}\ m^2/N$
S_{11}	1840	1370	0.98
S_{12}	-290	-148	-0.16
S_{13}	-120	-	-0.33
S_{33}	1020	-	27.5
S_{44}		3030	240.0

In terms of elastic constants (the inverse) the relationship is given by:

$$\begin{aligned} T_{xx} &= C_{11}e_{xx} + C_{12}e_{yy} + C_{13}e_{zz} \\ T_{yy} &= C_{12}e_{xx} + C_{11}e_{yy} + C_{13}e_{zz} \\ T_{zz} &= C_{13}e_{xx} + C_{13}e_{yy} + C_{33}e_{zz} \\ T_{zx} &= C_{44}e_{zx} \\ T_{zy} &= C_{44}e_{zy} \\ T_{xy} &= \frac{1}{2}(C_{11} - C_{12})e_{xy} \end{aligned} \qquad \ldots\ldots\ 33$$

Irradiating pyrolytic graphite and Ticonderoga flakes showed that only the C_{33} and C_{44} compliances changed; C_{33} tended to reduce and C_{44} to increase to a much larger degree to values associated with a perfect crystal.

The elastic moduli C_{33} and C_{44} are associated with the inter layer forces which may be expected to reduce as inter layer spacing increases. The reduction in C_{33} can readily be explained this way. However it has been shown that the large and material increase in C_{44} is associated with pinning of the glissile dislocations in the basal planes which would normally be responsible for a decrease in the shear constants.

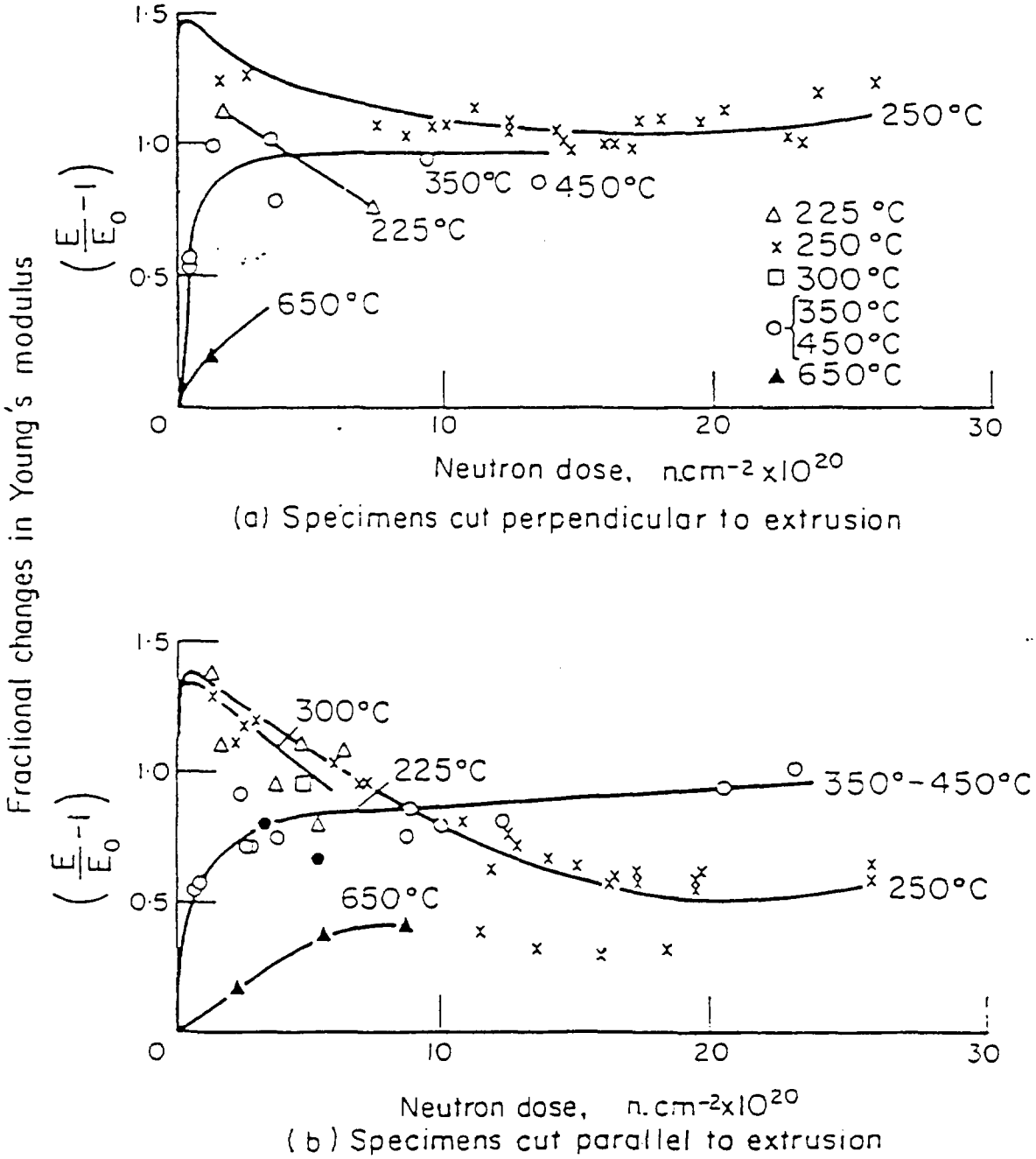

FIGURE 12: CHANGES IN YOUNG'S MODULAS OF A PILE GRADE 'A' GRAPHITE WITH NEUTRON DOSE

Fractional changes in Young's modulus for Pile Grade A graphite are given in Fig. 12. They show two distinct regions: Below 300°C the Young's modulus increases by a factor of about three, peaks and then decreases, followed by an increase and later a catastrophic decrease and disintegration. Above 300°C there is an initial increase which decreases with increasing temperature, a constant region and final fall.

The explanation for this behaviour is that, for low doses at temperatures below 300°C, pinning of the dislocations leads to an increase of modulus. The decrease in modulus that follows is due to large separation in the basal plane. Above 300° C there is the same temperature dependent increase due to pinning. Further irradiations above and below 300°C lead to an increase in modulus due to structural changes. The final decrease in modulus is due to large increases in porosity.

4.1. Irradiation creep

Simmons[1] showed that samples irradiated under stress showed different dimensional changes to those irradiated unstressed. Since then detailed studies of dimensional change under stresses have been carried out by many authors. Early tests in the Calder Hall Magnox reactor in the region 140°C to 324°C showed the effect was the same independent of temperature. It was also soon apparent that irradiation creep was a complex phenomenon as it was seen that the thermal expansion coefficients were increased by compressive creep strain. Measurement in lateral strain ratios varied from 0.3 to 0.5.

Kelly and Brocklehurst (1977) summarised creep studies carried out in the UK since 1946. They found that creep strain ε_c could be summarised for the temperature range between 140°C - 650°C by:

$$\varepsilon_c = 0.23\frac{\sigma}{E_o}\gamma + \frac{\sigma}{E_0}\left(1 - exp[-4\gamma]\right) \qquad 34$$

where σ (MPa)is the stress, γ is the dose (n/cm^2 EDND) and E_o is the static Young's modulus prior to irradiation, see Fig. 13.

The first term is the secondary creep strain and the second the transient creep strain. It should be noted than that both terms are inversely proportional to modulus. The creep rate increases slowly at higher temperatures and this was allowed for by the introduction of a temperature factor $\beta(T)$, which is unity below 650°C.

Poisson's ratio in creep was found to be 0.3 from a series of experiments and data was obtained on the changes in thermal expansion coefficient with creep strain. It was also clear that the transient creep strain was recoverable in the presence of thermal annealing.

It was shown that tensile creep strain decreased the thermal expansion coefficient measured parallel to the stress direction, while compressive creep strain increased the thermal expansion coefficient, see Fig. 14.

It was also interesting that boron doping of polycrystalline graphite, carried out to increase the fast neutron damage rate, did not increase the creep strain rate, pointing to the effect being dependent on atomic displacement rate only.

It is clear that creep of graphite is more complex than initially thought. This is particularly evident when considering the changes to thermal expansion coefficient

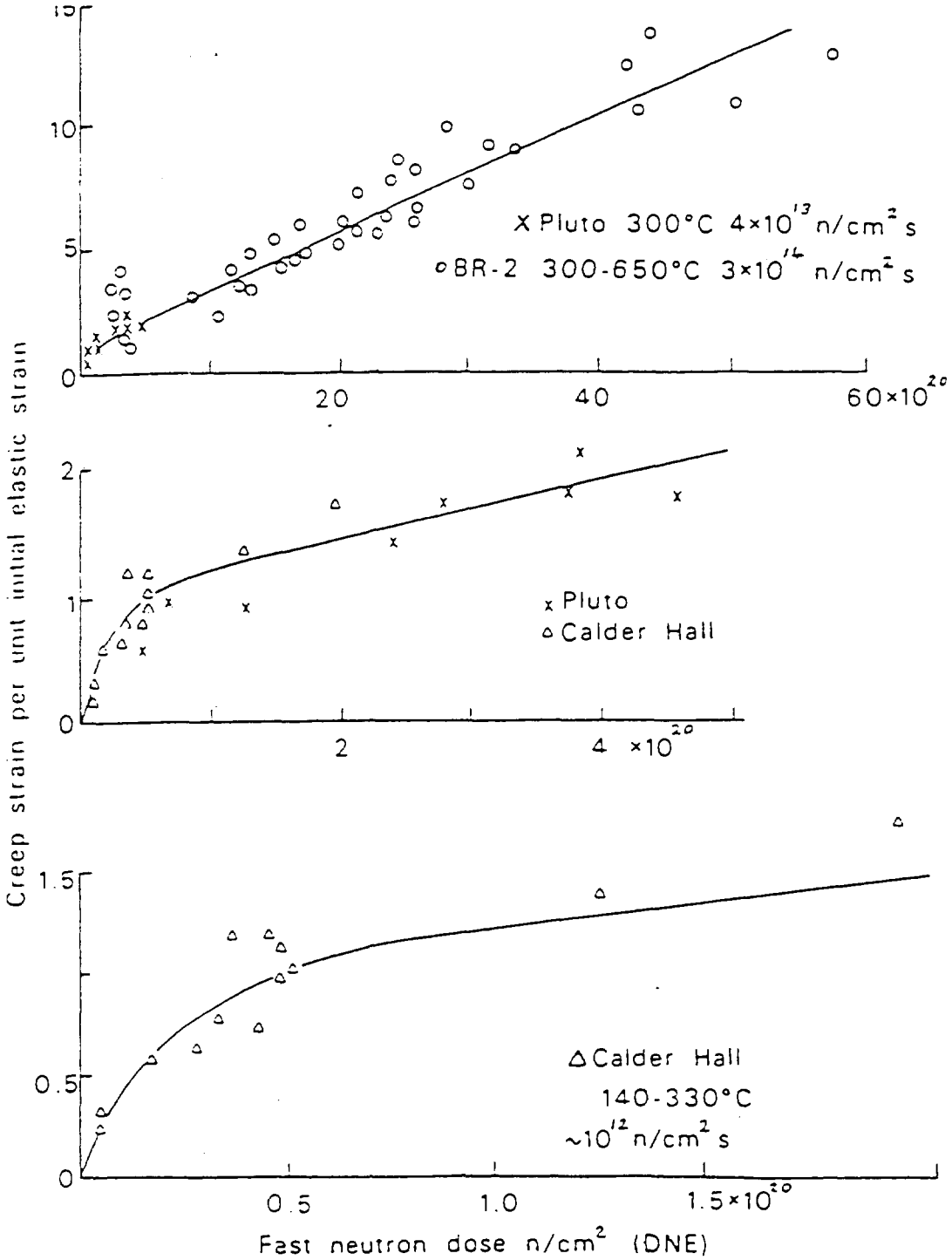

FIGURE 13: COMPARISON OF CONSTANT STRESS IRRADIATION CREEP DATA ON GRAPHITE IN DIFFERENT FACILITIES.

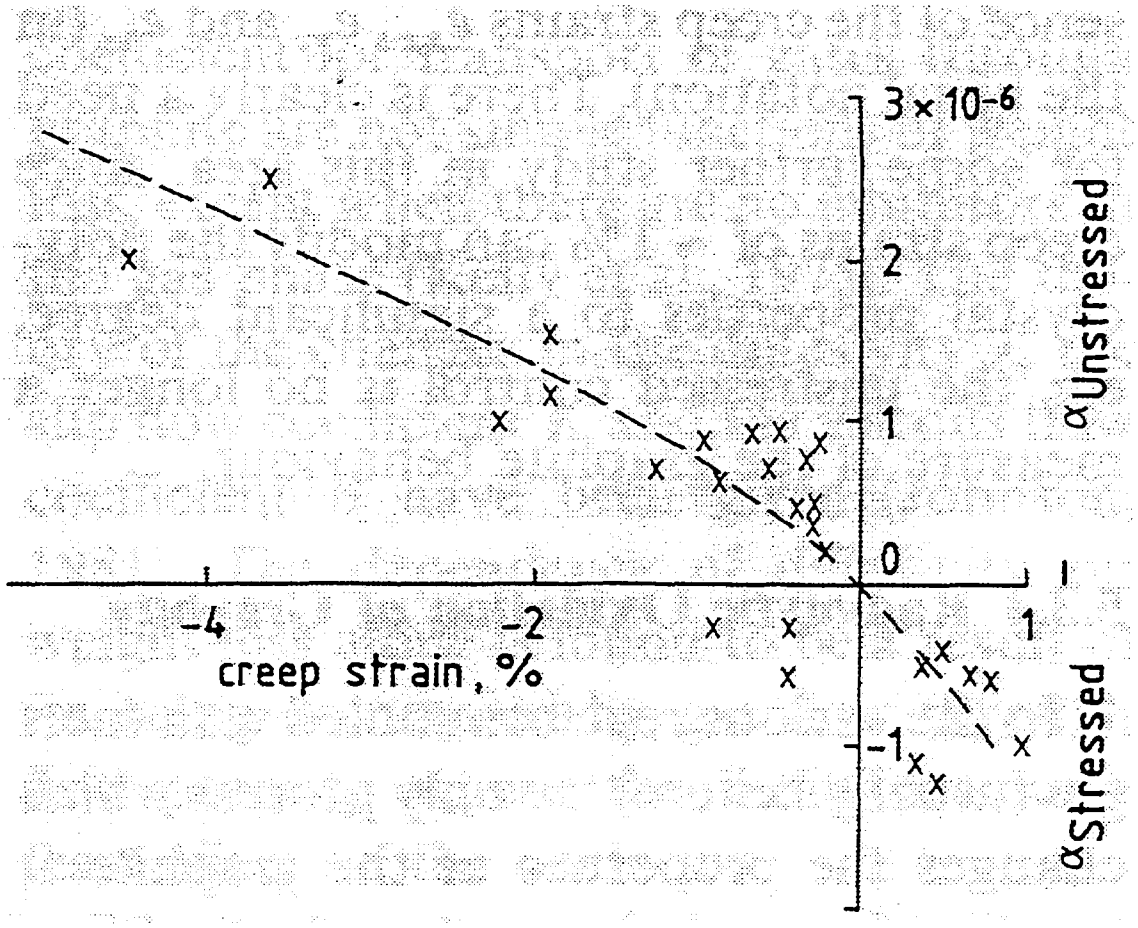

FIG 14: CREEP STRAIN TO THERMAL EXPANSION COEFFICIENT

with creep strain. We have already seen that changes in thermal expansion coefficient are related to dimensional change rates.

Two explanations can be put forward for the changes in thermal expansion coefficient; firstly due to the change in porosity due to creep strain, secondly due to the crystallite re-orientation due to creep strain. There is some evidence for the second process but it is possible that both processes occur.

Creep strains have conventionally been defined as the difference in strain between stressed and unstressed samples. This is not correct once significant changes in thermal expansion have occurred. It is readily shown that the true creep strain is:

$$\varepsilon_c' = \varepsilon_c + \int_0^{\gamma} \frac{(\alpha'_x - \alpha_x)}{(\alpha_c - \alpha_a)} \left(\frac{1}{X_c} \frac{dX_c}{d\gamma} - \frac{1}{X_a} \frac{dX_a}{d\gamma} \right) d\gamma \qquad 35$$

where ε_c is the conventional creep strain, α'_x is the thermal expansion coefficient of the crept sample and α_x is that of the control.

This effect is particularly important in the multi-axis case where the separation into creep and dimensional changes cannot be made and stress calculations become less accurate. In particular there must be a 'Poisson's' ratio effect for the change in thermal expansion coefficient with creep strain.

Recent experiments have been initiated to study this effect, by inducing large elastic strains into unirradiated graphite both in compression and tension, then measuring the change in thermal expansion. This work is still underway, however unexpectedly these experiments have shown that small elastic strains can produce similar changes in magnitude in the thermal expansion coefficient as was produced by the large creep strain.

It is clear that further work is required in this area particularly on irradiated graphites.

5. DISCUSSION

This paper has outlined only part of the vast amount of work that has been undertaken since the early 1940s. It is hoped to publish the work of Professor B.T.Kelly in more detail in the near future.
Whilst there is a well established understanding of the process of fast neutron damage in fission systems, more work, both experimental and theoretical, is required for higher energy systems such as first wall protection tiles in fusion systems where inelastic effects and transmutation may be significant.

Detailed structural analysis has been carried out on both UK and US graphites using the theory related to dimensional changes, thermal changes and mechanical changes. It would be useful to apply the same theories to other graphites where data is available. It is desirable to operate graphite moderated reactors beyond their original design life, therefore it is important to understand the behaviour of graphites to high irradiation doses. The application and extension of this theory can make a significant contribution to this task.

Detailed study of stored energy accumulation at low temperatures was discontinued in the late 1950s as the problem was designed out of the then new generations of graphite moderated reactors. However now attention has turned to the decommissioning of such systems and the theory is being revisited in order to make safety cases for dismantling and disposal of early graphite cores.

Further investigation is required into the interaction of strain, the coefficient of thermal expansion, dimensional change and elastic strain.

Finally graphite moderated reactors for both fission and fusion systems will be operating for many years into the future. It is therefore important that the vast amount of knowledge gained since the 1940s is not lost.

REFERENCES

1. Simmons J H W. "Radiation Damage in Graphite". Pergamon Press. (1965).
2. Kinchin G H and Pease R S. rep Progress in Physics Vol 18, p1. (1955).
3. Bell J C, Bridge H, Cottrell A H, Greenhough GB, Simmons J H W, and Reynolds W N, Phil Trans Roy Soc. A Vol 66, p961 (1962).
4. Wright S B "Radiation Damage in Solids". Vol 11,p239. IAEA Vienna. (1962).
5. IAEA-Specialists Meeting on Radiation Damage Units for Graphite, Seattle. (1972).
6. Linhard J and Scharff M. Phys Rev Vol 124, p128. (1964).
7. Kelly B.T., Martin W.H., Nettley P.T. Phil Trans. Royal Soc. Series A No. 1109, Vol. 260 pp 37-71 1966.
8. Bridge. H., Kelly B.T., Gray B.S. Stored energy and dimensional changes in reactor graphite. Proc. 5th Conf. on Carbon. Pergamon Press. 1962
9. Cotterell A.H., Lomer W.M., Simmons J.H.W., Bell J.C. Greenough G.B. A. Conf. Theory of annealing kinetics applied to the release of stored energy from irradiated graphite in air cooled reactors. 15/P2485. Second United Nations Conference on the Peaceful Uses of Atomic Energy. September 1958.
10. Vand V. Proc. Phy. Soc. A55, 222, (1943)
11. Primak W. Kinetics of processes distributed in activation energy. Phy. Rev. Vol 100, 6, Dec. 1955
12. Kelly B.T. Irradiation damage to solids Pergamon press, 1966
13. Kelly B.T. Physics of graphite, Applied Science Publishers, 1981